Spin symmetry and pseudospin symmetry in the relativistic mean field with a deformed potential

K. Sugawara-Tanabe,[1,2] S. Yamaji,[2] and A. Arima[3]
[1]*Otsuma Women's University, Karakida, Tama, Tokyo 206-8540, Japan*
[2]*RIKEN, Hirosawa, Wako, Saitama 351-0198, Japan*
[3]*House of Councilors, Nagatacho, Chiyoda-ku, Tokyo 100-8962, Japan*
(Received 3 December 2001; published 1 May 2002)

The equations for the pseudospin pair levels become of the same form as those of the spin pair levels at the limit where the derivatives of potentials are zero. However, the centrifugal terms of four amplitudes among eight components in the pseudospin pair levels have pseudo-$\tilde{l}_z$, while those in the spin pair-levels have natural l_z. When both of the pseudospin and spin symmetries are well satisfied, there appears a triple degeneracy. The relativistic mean-field calculation over ^{154}Sm gives [400]1/2, [402]3/2, and [402]5/2 levels as such a candidate. The relation between the deformed wave function and the spherical wave function are discussed at the spherical limit by using the transformation from the cylindrical coordinate into the polar coordinate.

DOI: 10.1103/PhysRevC.65.054313 PACS number(s): 21.10.Pc, 21.10.Hw, 21.60.Jz, 21.30.−x

I. INTRODUCTION

One of the advantages in the relativistic treatment is that it clarifies the origin of the spin-orbit interaction, which is also related with the pseudospin concept [1,2]. Recently, there appeared various research papers with the purpose to find the root of the pseudospin concept to the relativistic mean-field equation [3–9]. We found the general and realistic conditions for the pseudospin approximation both for the spherical potential [6–8], and the deformed potential [7,9]. It has been discovered that the condition found in the large component of Dirac wave function works much better than that in the small component wave function for the deformed case in contrast to the spherical case [9].

The pseudospin concept in the deformed nuclei is defined in the nonrelativistic treatment [10] as following: The single-particle levels with $j_z=\Omega=l_z+1/2$ and $j_z'=\Omega+1=l_z+2-1/2$ lie very close in energy, and these two levels are labeled as $j_z=\tilde{l}_z-1/2$ and $j_z'=\tilde{l}_z+1/2$ with $\tilde{l}_z=l+1$. If we use the asymptotic quantum number $[N,n_z,l_z]\Omega$ with $j_z=\Omega$ to identify the deformed state, which is usually used in the nonrelativistic calculation, the pseudospin pair levels become $[N,n_z,l_z]\Omega$ and $[N,n_z,l_z+2](\Omega+1)$, or equivalently $[N,n_z,\tilde{l}_z](\tilde{l}_z-1/2)$ and $[N,n_z,\tilde{l}_z](\tilde{l}_z+1/2)$. On the other hand, the spin pair-levels are labeled by $[N,n_z,l_z]\Omega$ and $[N,n_z,l_z](\Omega+1)$, or equivalently $[N,n_z,l_z](l_z-1/2)$ and $[N,n_z,l_z](l_z+1/2)$, as they are split only by the spin-orbit interaction.

The conditions we have found for the pseudospin symmetry in our previous work [Eqs. (2.8) and (2.10) in Ref. [9]] seem also to work for the spin symmetry. Moreover, we found the revival of L-S coupling scheme at superdeformation in the nonrelativistic calculation, showing that the expectation values of spin-orbit interaction decreases with increasing deformation for small Ω [11]. Thus, we compare the pseudospin pair levels with $\tilde{l}_z\pm1/2$, and the spin pair levels with $l_z\pm1/2$ by using the relativistic mean-field program [12] for ^{154}Sm in this paper. In Sec. II our theory is reviewed, in Sec. III the realtion between the spherical wave function and the deformed wave function is discussed. In Sec. IV the numerical analysis is carried out on ^{154}Sm, and the conclusion is given in Sec. V.

II. THEORY

The eigenfunction $\psi(\vec{r})$ for the Dirac equation with an axially symmetrically deformed potential has two components, i.e., upper (large) component g and lower (small) component f. We use the cylindrical coordinates (ρ,φ,z), and then each of g and f in $\psi(\vec{r})$ has two components,

$$g=\frac{1}{\sqrt{2\pi}}\begin{pmatrix} ig^{\Omega}_{+,k}e^{i(\Omega-1/2)\varphi} \\ ig^{\Omega}_{-,k}e^{i(\Omega+1/2)\varphi}\end{pmatrix},$$

$$f=\frac{1}{\sqrt{2\pi}}\begin{pmatrix} f^{\Omega}_{+,k}e^{i(\Omega-1/2)\varphi} \\ f^{\Omega}_{-,k}e^{i(\Omega+1/2)\varphi}\end{pmatrix}. \tag{2.1}$$

Here $g^{\Omega}_{\pm,k}$ and $f^{\Omega}_{\pm,k}$ are functions of ρ and z, k denotes the other quantum numbers except for Ω. The $\pm$ sign in $g^{\Omega}_{\pm,k}$ and $f^{\Omega}_{\pm,k}$ corresponds to the spin wave function with $s_z=\pm1/2$. Inserting this equation into the Dirac equation, we get the coupled equations. We then found the equations for $g^{\Omega}_{\pm,k}$ and the equations for $f^{\Omega}_{\pm,k}$ have a form symmetric to each other [7,9]

$$\begin{aligned}-V_1V_2g^{\Omega}_{\pm,k}=&\left[\partial_\rho^2-\frac{(\Omega\mp1/2)^2}{\rho^2}+\frac{\partial_\rho}{\rho}+\partial_z^2\right]g^{\Omega}_{\pm,k}\\&-\frac{\partial_\rho V_2}{V_2}\left[\left(\partial_\rho\mp\frac{\Omega\mp1/2}{\rho}\right)g^{\Omega}_{\pm,k}\mp\partial_z g^{\Omega}_{\mp,k}\right]\\&-\frac{\partial_z V_2}{V_2}\left[\left(\pm\partial_\rho+\frac{\Omega\pm1/2}{\rho}\right)g^{\Omega}_{\mp,k}+\partial_z g^{\Omega}_{\pm,k}\right],\end{aligned} \tag{2.2}$$

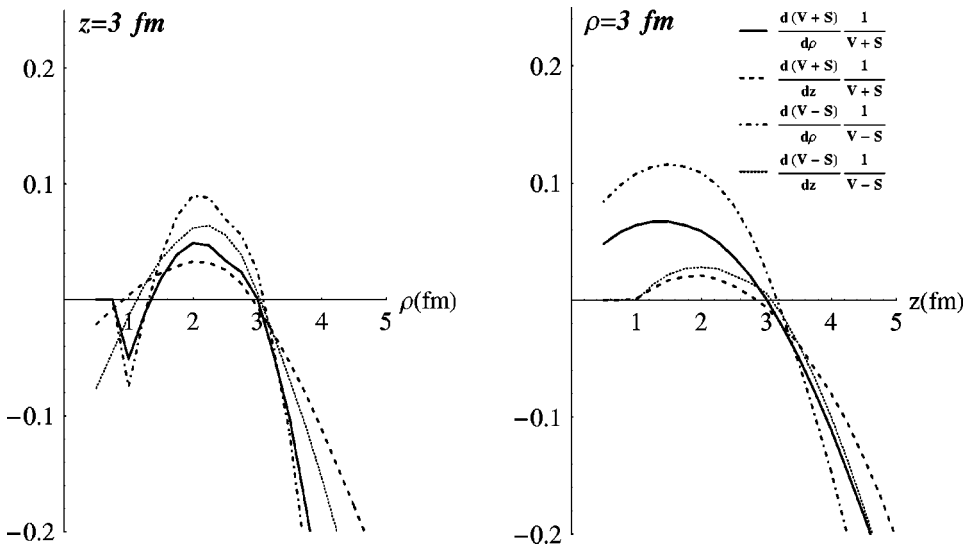

FIG. 1. The ratio of the potential derivatives to the potentials as a function of ρ at $z=3$ fm (left panel), and as a function of z at $\rho=3$ fm (right panel). V corresponds to V_V and S to V_S in the text.

$$-V_1V_2f^{\Omega}_{\pm,k}=\left[\partial_\rho^2-\frac{(\Omega\mp1/2)^2}{\rho^2}+\frac{\partial_\rho}{\rho}+\partial_z^2\right]f^{\Omega}_{\pm,k}-\frac{\partial_\rho V_1}{V_1}\left[\left(\partial_\rho\mp\frac{\Omega\mp1/2}{\rho}\right)f^{\Omega}_{\pm,k}\mp\partial_z f^{\Omega}_{\mp,k}\right]-\frac{\partial_z V_1}{V_1}\left[\left(\pm\partial_\rho+\frac{\Omega\pm1/2}{\rho}\right)f^{\Omega}_{\mp,k}+\partial_z f^{\Omega}_{\pm,k}\right]. \tag{2.3}$$

Here $\partial_\rho^2=\partial^2/\partial\rho^2$, $\partial_\rho=\partial/\partial\rho$, $\partial_z^2=\partial^2/\partial z^2$, and $\partial_z=\partial/\partial z$. The eigenvalue of Dirac equation ϵ is included in two kinds of potentials V_1 and V_2,

$$V_1=M-\epsilon_{k,\Omega}-V_S-V_V,\quad V_2=\epsilon_{k,\Omega}+M+V_S-V_V, \tag{2.4}$$

with vector potential V_V, scalar potential V_S, and mass M. As seen in Eqs. (2.2) and (2.3), $g^{\Omega}_{\pm,k}$ and $f^{\Omega}_{\pm,k}$ have symmetric forms by exchanging V_2 by V_1. It is also seen from Eqs. (2.2) and (2.3) that there exists a symmetry relation among $g^{\Omega}_{\pm,k}$ ($f^{\Omega}_{\pm,k}$) and $g^{-\Omega}_{\pm,k}$ ($f^{-\Omega}_{\pm,k}$) in the axially symmetrically deformed case coming from the time reversal invariance. From now on, we will limit our discussion to the positive value of Ω and use both $f^{\Omega}_{\pm,k}$ and $g^{\Omega}_{\pm,k}$.

Let us assume the case where the following conditions are satisfied:

$$\partial V_2/\partial\rho=0,\quad \partial V_2/\partial z=0. \tag{2.5}$$

In this special region, the coupled equation (2.2) becomes

$$-V_1V_2g^{\Omega}_{-,k}=\left[\partial_\rho^2-\frac{(\Omega+1/2)^2}{\rho^2}+\frac{\partial_\rho}{\rho}+\partial_z^2\right]g^{\Omega}_{-,k},$$
$$-V_1'V_2'g^{\Omega+1}_{+,k'}=\left[\partial_\rho^2-\frac{(\Omega+1/2)^2}{\rho^2}+\frac{\partial_\rho}{\rho}+\partial_z^2\right]g^{\Omega+1}_{+,k'}, \tag{2.6}$$

where V_1 and V_2 have $\epsilon_{k,\Omega}$, while V_1' and V_2' have $\epsilon_{k',\Omega+1}$ as is defined in Eq. (2.4). This is nothing but the pseudospin doublets, if k corresponds to $[N,n_z,l_z]$, k' to $[N,n_z,l_z'=l_z+2]$, and $\epsilon_{k,\Omega}\sim\epsilon_{k',\Omega+1}$ or $V_1=V_1'$ and $V_2=V_2'$. They obey the same equation with $\tilde{l}_z=\Omega+1/2$ in the centrifugal term. However, they have *unnatural* l_z, because the true value of l_z for the former level must be $l_z=\Omega-1/2$ as $j_z=\Omega=l_z+1/2$, and the true value of l_z' for the latter level is $l_z'=\Omega+3/2$ as $j_z'=\Omega+1=l_z+2-1/2$. According to the definition in Ref. [9], we called them *unphysical* amplitudes. From now on we will call them the amplitudes with *unnatural* l_z.

If both of k and k' are the same with $[N,n_z,l_z]$, and $\epsilon_{k,\Omega}$ nearly equals $\epsilon_{k,\Omega+1}$, Eq. (2.6) also corresponds to the spin doublets, as $\Omega=l_z-1/2$ and $\Omega+1=l_z+1/2$. In this case, spin doublets have *natural* $l_z=\Omega+1/2$ in the centrifugal term. We called them *physical* amplitudes in Ref. [9]. In this paper we will call them the amplitudes with *natural* l_z. We must pay attention to the fact that the condition (2.5) is effective in both pseudospin doublets and spin doublets.

It is found that the region where $\partial_\rho V_1=0$ overlaps the region where $\partial_\rho V_2=0$, and the region where $\partial_z V_1=0$ overlaps the region where $\partial_z V_2=0$ (see Figs. 2 and 3 in Ref. [9]). In Fig. 1, we confirmed that the region where $\partial_\rho V_2=0$ equals the region where $\partial_z V_2=0$, $\partial_\rho V_1=0$, and $\partial_z V_1=0$. We can apply the same discussion to the lower components as that to the upper components. If the following condition is satisfied:

$$\partial_\rho V_1=0,\quad \partial_z V_1=0, \tag{2.7}$$

then

$$-V_1V_2f^{\Omega}_{-,k}=\left[\partial_\rho^2-\frac{(\Omega+1/2)^2}{\rho^2}+\frac{\partial_\rho}{\rho}+\partial_z^2\right]f^{\Omega}_{-,k},$$
$$-V_1'V_2'f^{\Omega+1}_{+,k'}=\left[\partial_\rho^2-\frac{(\Omega+1/2)^2}{\rho^2}+\frac{\partial_\rho}{\rho}+\partial_z^2\right]f^{\Omega+1}_{+,k'}. \tag{2.8}$$

If k corresponds to $[N,n_z,l_z]$, and k' to $[N,n_z,l_z+2]$, $f^{\Omega}_{-,k}$ and $f^{\Omega+1}_{+,k'}$ for the pseudospin doublets ($\epsilon_{k,\Omega}\sim\epsilon_{k',\Omega+1}$), obey the same equation with $\tilde{l}_z$. In other words, the pseudospin doublet is found in the amplitudes with *unnatural* l_z of lower components. If both k and k' are defined as $[N,n_z,l_z]$,

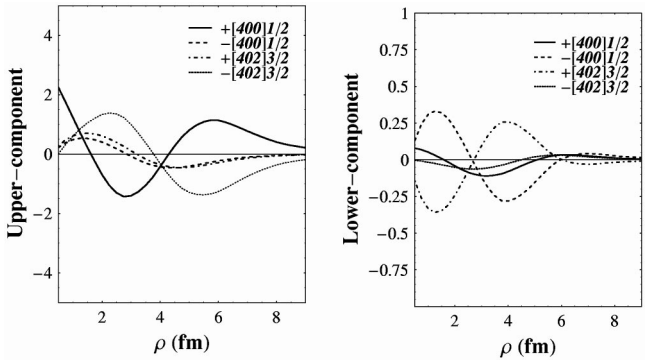

FIG. 2. The upper components (left panel) and lower components (right panel) for pseudospin doublet of [400]1/2 and [402]3/2 as a function of ρ at $z=3$ fm. The dashed and the dot-dashed lines are for the *unphysical* amplitudes, and the solid and the dotted lines are for the *physical* amplitudes. The dashed and solid lines are for [400]1/2 and the dot-dashed and the dotted lines are for [402]3/2. The $\pm$ sign in front of $[N,n_z,l_z]\Omega$ corresponds to $\pm\frac{1}{2}$ of s_z.

$f^{\Omega}_{-,k}$ and $f^{\Omega+1}_{+,k}$ for the spin doublets ($\epsilon_{k,\Omega}\sim\epsilon_{k,\Omega+1}$) have *natural* $l_z=\Omega+1/2$ in the centrifugal term. In other words, the spin doublets are found in the amplitudes with natural l_z of lower components. Again, the condition (2.7) that is satisfied in the same region as Eq. (2.5), works both for the pseudospin doublets and spin doublets.

Now we consider of the other amplitudes for the states with (k,Ω) and $(k',\Omega+1)$, i.e., $g^{\Omega}_{+,k}$ ($f^{\Omega}_{+,k}$) and $g^{\Omega+1}_{-,k'}$ ($f^{\Omega+1}_{-,k'}$). Under the same conditions of Eq. (2.5) or Eq. (2.7), they become

$$-V_1V_2g^{\Omega}_{+,k}=\left[\partial_\rho^2-\frac{(\Omega-1/2)^2}{\rho^2}+\frac{\partial_\rho}{\rho}+\partial_z^2\right]g^{\Omega}_{-,k},$$

$$-V_1'V_2'g^{\Omega+1}_{-,k'}=\left[\partial_\rho^2-\frac{(\Omega+3/2)^2}{\rho^2}+\frac{\partial_\rho}{\rho}+\partial_z^2\right]g^{\Omega+1}_{-,k'},$$

$$-V_1V_2f^{\Omega}_{+,k}=\left[\partial_\rho^2-\frac{(\Omega-1/2)^2}{\rho^2}+\frac{\partial_\rho}{\rho}+\partial_z^2\right]f^{\Omega}_{-,k},$$

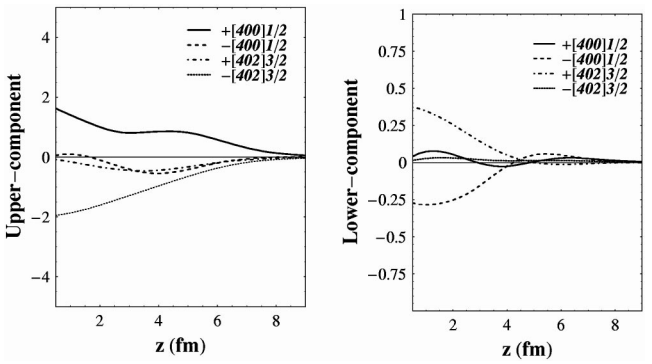

FIG. 3. The upper components (left panel) and lower components (right panel) for pseudospin doublet of [400]1/2 and [402]3/2 as a function of z at $\rho=5$ fm. The lines are the same as defined in Fig. 2.

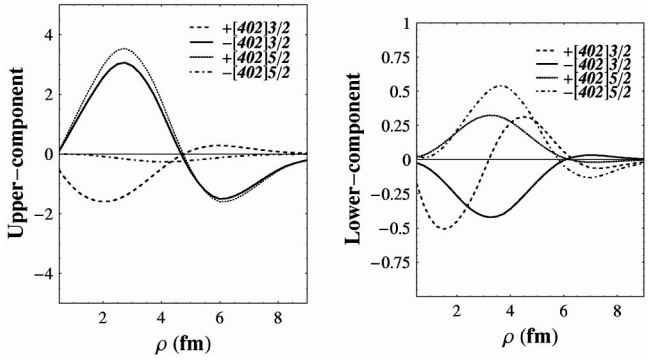

FIG. 4. The upper components (left panel) and lower components (right panel) for spin doublet of [402]3/2 and [402]5/2 as a function of ρ at $z=1$ fm. The lines for the *unphysical* and *physical* amplitudes are the same as defined in Fig. 2. The dashed and the solid lines are for [402]3/2 and the dot-dashed and the dotted lines are for [402]5/2.

$$-V_1'V_2'f^{\Omega+1}_{-,k'}=\left[\partial_\rho^2-\frac{(\Omega+3/2)^2}{\rho^2}+\frac{\partial_\rho}{\rho}+\partial_z^2\right]f^{\Omega+1}_{-,k'}. \tag{2.9}$$

These amplitudes have *natural* l_z and l_z+2 for the pseudospin doublets of $k=[N,n_z,l_z]$ and $k'=[N,n_z,l_z+2]$. They obey different equations except for large ρ where the contribution from the centrifugal term becomes negligible. The pseudospin doublets with $g^{\Omega}_{+,k}$ ($f^{\Omega}_{+,k}$) of $k=[N,n_z,l_z]$ and $g^{\Omega+1}_{-,k'}$ ($f^{\Omega+1}_{-,k'}$) of $k'=[N,n_z,l_z+2]$ obey the different equation but with *natural* l_z. If we choose $k=k'=[N,n_z,l_z]$ in Eq. (2.9), these amplitudes have *unnatural* l_z. For the spin doublets with $k=[N,n_z,l_z]$, $g^{\Omega}_{+,k}$($f^{\Omega}_{+,k}$) and $g^{\Omega+1}_{-,k}$ ($f^{\Omega+1}_{-,k}$) obey the different equation with *unnatural* l_z.

From Figs. 2 to 5, we have compared these eight amplitudes for both pseudospin doublets and spin doublets. In all the figures, the amplitudes with *unnatural* l_z are shown by dashed or dot-dashed lines, while the amplitudes with *natural* l_z are shown by solid or dotted lines. Both the dashed and the solid lines correspond to the level with Ω, and both the dot-dashed and dotted lines correspond to the level with $(\Omega+1)$. The numerical analysis that supports Eqs. (2.6) and

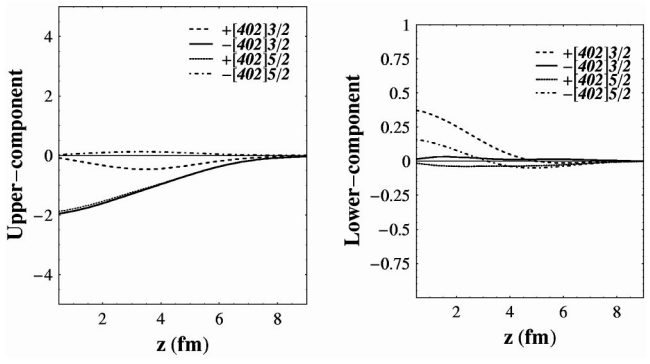

FIG. 5. The upper components (left panel) and lower components (right panel) for spin doublet of [402]3/2 and [402]5/2 as a function of z at $\rho=5$ fm. The lines are the same as defined in Fig. 4.

(2.8) works well for the case where the pseudospin symmetry and the spin symmetry become better. If there were a good degeneracy in the pair levels labeled with (k,Ω) and $(k',\Omega+1)$, and also with $(k',\Omega+1)$ and $(k',\Omega+2)$, there would appear triple degeneracy. In the realistic case, it is hard to appear, but Figs. 2–5 seem to show such candidate possibilities.

III. THE RELATION TO THE SPHERICAL CASE

Now we will discuss the relation between the deformed case and the spherical case. At the spherical limit, we have used the polar coordinate (r,θ,φ) instead of the cylindrical coordinate [6–8]. The upper and lower components in the spherical limit are denoted by

$$g = i\frac{G^{lj}(r)}{r}\mathcal{Y}^l_{jm}(\theta,\phi),$$

$$f = \frac{F^{lj}(r)}{r}(\vec{\sigma}\cdot\hat{r})\mathcal{Y}^l_{jm}(\theta,\phi), \tag{3.1}$$

where $\mathcal{Y}^l_{jm}(\theta,\phi)$ is a vector spherical harmonics. We rewrite Eq. (2.1) by replacing $k=[l,j]$ and then comparing it with Eq. (3.1). Then, we get the relation between $f^{\Omega}_{\pm,l,j=l\pm1/2}(r,\theta)$ and $g^{\Omega}_{\pm,l,j=l\pm1/2}(r,\theta)$, and $G^{l,j=l\pm1/2}(r)$ and $F^{l,j=l\pm1/2}(r)$.

$$f^{\Omega}_{\pm,l,j=l+1/2}(r,\theta) = \pm\sqrt{2\pi}e^{-i(\Omega\mp1/2)\varphi}\sqrt{\frac{l+3/2\mp\Omega}{2l+3}} \times Y^{l+1}_{\Omega\mp1/2}(\theta,\varphi)\frac{F^{l,j=l+1/2}(r)}{r},$$

$$f^{\Omega}_{\pm,l,j=l-1/2}(r,\theta) = -\sqrt{2\pi}e^{-i(\Omega\mp1/2)\varphi}\sqrt{\frac{l-1/2\pm\Omega}{2l-1}} \times Y^{l-1}_{\Omega\mp1/2}(\theta,\varphi)\frac{F^{l,j=l-1/2}(r)}{r},$$

$$g^{\Omega}_{+,l,j=l\pm1/2}(r,\theta) = \pm\sqrt{2\pi}e^{-i(\Omega-1/2)\varphi}\sqrt{\frac{l+1/2\pm\Omega}{2l+1}} \times Y^{l}_{\Omega-1/2}(\theta,\varphi)\frac{G^{l,j=l\pm1/2}(r)}{r},$$

$$g^{\Omega}_{-,l,j=l\pm1/2}(r,\theta) = \sqrt{2\pi}e^{-i(\Omega+1/2)\varphi}\sqrt{\frac{l+1/2\mp\Omega}{2l+1}} \times Y^{l}_{\Omega+1/2}(\theta,\varphi)\frac{G^{l,j=l\pm1/2}(r)}{r}. \tag{3.2}$$

Here $f^{\Omega}_{\pm,l,j=l\pm1/2}(r,\theta)$ and $g^{\Omega}_{\pm,l,j=l\pm1/2}(r,\theta)$ are functions of (r,θ) and not (ρ,z), and $Y^l_{\Omega}(\theta,\varphi)$ is the spherical harmonics.

In the spherical limit, it is said that the pseudospin symmetry is hidden in the lower component [3,4,6–8], while the spin symmetry is in the upper component. From Eq. (3.2), we see the following relations:

$$\frac{f^{\Omega+1}_{+,l+2,j=l+2-1/2}(r,\theta)}{f^{\Omega}_{-,l,j=l+1/2}(r,\theta)} = \frac{F^{l+2,j=l+2-1/2}(r)}{F^{l,j=l+1/2}(r)}\frac{\sqrt{l+5/2+\Omega}}{\sqrt{l+3/2+\Omega}}$$

$$\frac{g^{\Omega+1}_{+,l,j=l+1/2}(r,\theta)}{g^{\Omega}_{-,l,j=l-1/2}(r,\theta)} = \frac{G^{l,j=l+1/2}(r)}{G^{l,j=l-1/2}(r)}\frac{\sqrt{l+3/2+\Omega}}{\sqrt{l+1/2+\Omega}}. \tag{3.3}$$

There is no simple relation among the ratio for $g^{\Omega+1}_{+,l+2,j=l+2-1/2}(r,\theta)$ and $g^{\Omega}_{-,l,j=l+1/2}(r,\theta)$, and also for $f^{\Omega+1}_{+,l,j=l+1/2}(r,\theta)$ and $f^{\Omega}_{-,l,j=l-1/2}(r,\theta)$. It indicates that if we choose polar coordinate at the spherical limit, $f^{\Omega}_{\pm,l,j}(r,\theta)$ has pseudospin symmetry while $g^{\Omega}_{\pm,l,j}(r,\theta)$ has spin symmetry in itself.

To make our discussion much clearer, we return to the original definition of $g^{\Omega}_{\pm,k}$ and $f^{\Omega}_{\pm,k}$ at the spherical limit without using the representation by r and θ. The relation between the cylindrical coordinate and polar coordinate gives $\partial_r V_1 = \cos\theta\partial_z V_1 + \sin\theta\partial_\rho V_1$, which shows that if condition (2.7) is satisfied, automatically $\partial_r V_1 = 0$, i.e., the condition for the pseudospin symmetry [6–8] at the spherical limit. As the potentials have no θ dependence at the spherical limit, $\rho\partial_z V_1 = z\partial_\rho V_1$ and $\rho\partial_z V_2 = z\partial_\rho V_2$, and the quantum number k is replaced by l and j. If $\epsilon_{l,j,\Omega} \sim \epsilon_{l+2,j+1,\Omega+1}$, we can derive the equation for the linear combination of the amplitudes with $\tilde{l}_z$ of the lower components in the pseudospin doublets from Eq. (2.3)

$$-V_1^2(f^{\Omega+1}_{+,l+2,j+1} \pm f^{\Omega}_{-,l,j}) = \frac{V_1}{V_2}\left(\partial_\rho^2 + \frac{\partial_\rho}{\rho} - \partial_z^2\frac{(\Omega+1/2)^2}{\rho^2}\right)(f^{\Omega+1}_{+,l+2,j+1} \pm f^{\Omega}_{-,l,j}) - \frac{\partial_\rho V_1}{V_2}\Bigg[\left(\partial_\rho + \frac{z}{\rho}\partial_z\right)(f^{\Omega+1}_{+,l+2,j+1} \pm f^{\Omega}_{-,l,j}) - \frac{\Omega+1/2}{\rho}(f^{\Omega+1}_{+,l+2,j+1} \mp f^{\Omega}_{-,l,j}) + \left(-\partial_z + \frac{z}{\rho}\partial_\rho\right)(f^{\Omega+1}_{-,l+2,j+1} \mp f^{\Omega}_{+,l,j}) + \frac{z}{\rho^2}\Omega(f^{\Omega+1}_{-,l+2,j+1} \pm f^{\Omega}_{+,l,j}) + \frac{z}{2\rho^2}(3f^{\Omega+1}_{-,l+2,j+1} \mp f^{\Omega}_{+,l,j})\Bigg]. \tag{3.4}$$

Either of the linear combination of $f^{\Omega+1}_{+,l+2,j+1} \pm f^{\Omega}_{-,l,j}$ ($-$ sign in Fig. 2 case) is larger than $f^{\Omega+1}_{-,l+2,j+1} \mp f^{\Omega}_{+,l,j}$ ($+$ sign in Fig. 2 case) for the pseudospin doublets. Moreover, V_2 is large and never goes to zero in its definition. Thus, we can neglect the third and the fourth lines in Eqs. (3.4). This implies that the pseudospin symmetry persists in the lower amplitudes at the spherical limit. Similarly, we rewrite Eq. (2.2) for the linear combination of the amplitudes with $\tilde{l}_z$ in the upper components for the pseudospin doublets,

$$
\begin{aligned}
-V_1(g^{\Omega+1}_{+,l+2,j+1} \pm g^{\Omega}_{-,l,j}) = & \frac{1}{V_2}\left(\partial_\rho^2 + \frac{\partial_\rho}{\rho} + \partial_z^2 - \frac{(\Omega+1/2)^2}{\rho^2}\right)(g^{\Omega+1}_{+,l+2,j+1} \pm g^{\Omega}_{-,l,j}) \\
& - \frac{\partial_\rho V_2}{V_2^2}\Bigg[\left(\partial_\rho + \frac{z}{\rho}\partial_z\right)(g^{\Omega+1}_{+,l+2,j+1} \pm g^{\Omega}_{-,l,j}) - \frac{\Omega+1/2}{\rho}(g^{\Omega+1}_{+,l+2,j+1} \mp g^{\Omega}_{-,l,j}) \\
& + \left(-\partial_z + \frac{z}{\rho}\partial_\rho\right)(g^{\Omega+1}_{-,l+2,j+1} \mp g^{\Omega}_{+,l,j}) + \frac{z}{\rho^2}\Omega(g^{\Omega+1}_{-,l+2,j+1} \pm g^{\Omega}_{+,l,j}) + \frac{z}{2\rho^2}(3g^{\Omega+1}_{-,l+2,j+1} \mp g^{\Omega}_{+,l,j})\Bigg].
\end{aligned}
\tag{3.5}
$$

As V_2 is much larger than V_1 and never becomes zero, we can neglect the terms proportional to $\partial_\rho V_2 / V_2^2$. As we see in Fig. 2, the amplitudes with *unnatural* l_z in the upper components are small for the pseudospin doublets. They may be small as to be of negligible order at the spherical limit. Moreover, the relation between the cylindrical coordinate and the polar coordinate gives $\partial_r V_2 = \cos\theta \partial_z V_2 + \sin\theta \partial_\rho V_2$. Subsequently, if condition (2.5) is satisfied, $\partial_r V_2 = 0$, which is not the condition for the pseudospin symmetry at the spherical limit as is proved in our previous work [7].

Next, we consider the linear combination of the amplitudes with *natural* l_z for the spin doublets at the spherical limit. If there were a good degeneracy of the spin doublets, i.e., $\epsilon_{l,j,\Omega} \sim \epsilon_{l,j+1,\Omega+1}$, the linear combination of the amplitudes with *natural* l_z in the upper components satisfies the equation

$$
\begin{aligned}
-V_1(g^{\Omega+1}_{+,l,j+1} \pm g^{\Omega}_{-,l,j}) = & \frac{1}{V_2}\left(\partial_\rho^2 + \frac{\partial_\rho}{\rho} + \partial_z^2 - \frac{(\Omega+1/2)^2}{\rho^2}\right)(g^{\Omega+1}_{+,l,j+1} \pm g^{\Omega}_{-,l,j}) \\
& - \frac{\partial_\rho V_2}{V_2^2}\Bigg[\left(\partial_\rho + \frac{z}{\rho}\partial_z\right)(g^{\Omega+1}_{+,l,j+1} \pm g^{\Omega}_{-,l,j}) - \frac{\Omega+1/2}{\rho}(g^{\Omega+1}_{+,l,j+1} \mp g^{\Omega}_{-,l,j}) \\
& + \left(-\partial_z + \frac{z}{\rho}\partial_\rho\right)(g^{\Omega+1}_{-,l,j+1} \mp g^{\Omega}_{+,l,j}) + \frac{z}{\rho^2}\Omega(g^{\Omega+1}_{-,l,j+1} \pm g^{\Omega}_{+,l,j}) + \frac{z}{2\rho^2}(3g^{\Omega+1}_{-,l,j+1} \mp g^{\Omega}_{+,l,j})\Bigg].
\end{aligned}
\tag{3.6}
$$

As we see in Fig. 4, either of the linear combination of $g^{\Omega+1}_{+,l,j+1} \pm g^{\Omega}_{-,l,j}$ ($+$ sign in Fig. 4) are larger than $g^{\Omega+1}_{-,l,j+1} \mp g^{\Omega}_{+,l,j}$ ($-$ sign in Fig. 5) for the spin doublets. Thus, we can neglect the terms proportional to $\partial_\rho V_2 / V_2^2$ in Eq. (3.6). This indicates that the spin symmetry exists in the upper components at the spherical limit, only when $\epsilon_{l,j,\Omega} \sim \epsilon_{l,j+1,\Omega+1}$. One gets a similar result for the lower components by replacing the index $(\pm, l+2, j+1)$ by $(\pm, l, j+1)$ in Eq. (3.4). As the amplitudes with *unnatural* l_z in lower components for the spin doublets are small, the spin symmetry is not seen in the lower components at the spherical limit.

In the spherical limit, the pseudospin symmetry is in the small component and the spin symmetry is in the large component, when they are expressed in the polar coordinate. In the deformed case, when they are expressed in the cylindrical coordinate, the pseudospin symmetry and the spin symmetry are found both in the upper (large) and lower (small) components. Both symmetries are closely related, which indicates that the deformed field mixes both symmetries just as the deformation mixes l and j. As the pseudospin symmetry is found not only in the small component but also in the large component, the pseudospin symmetry becomes better in the deformed nuclei than in the spherical nuclei.

IV. NUMERICAL ANALYSIS

We have performed the numerical analysis for ^{154}Sm with the same code and parameter set as in our previous work [9]. We have rewritten the relativistic Hartree plus BCS approximation code for the deformed nuclei developed by Ring's group [12].

1. Derivatives of the potentials with respect to ρ and z

In Fig. 1 we show the relative ratio of the potential derivatives with respect to ρ and z to the potentials $V_V \pm V_S$, which is shown by $V \pm S$ in the figure. From Eq. (2.4) the derivatives of V_1 and V_2 are the same as the derivatives of $V_V \pm V_S$. The figure shows that the region where four kinds of derivatives become zero are nearly the same. For much larger z and ρ, the derivatives of $V_V \pm V_S$ go to zero, as the potentials are conversing to zero, which is shown in Figs. 2

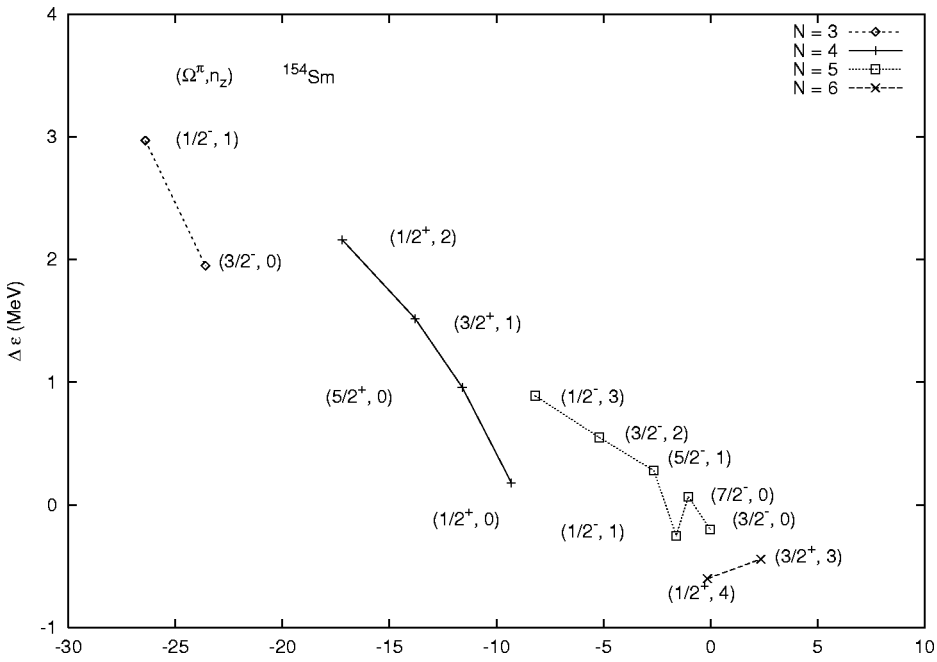

FIG. 6. The energy difference $\Delta\varepsilon$ vs average energy ε for the pseudospin pair levels. The longitudinal axis is for $\Delta\varepsilon$ and the horizontal axis is for ε defined in Eq. (4.1). The numerals inside parentheses are $(\Omega^{\text{parity}},n_z)$. The doublets belonging to $N=3$ are shown by diamonds, those to $N=4$ by pluses, those to $N=5$ by squares, and those to $N=6$ by crosses.

and 3 in Ref. [9]. Thus, the numerical analysis with a realistic parameter supports the observation that the conditions (2.5) and (2.7) are not independent, but are satisfied at the same region.

2. The wave functions for the pseudospin doublet

From Figs. 2 to 5 we show the wave functions for the pseudospin doublets (Figs. 2 and 3), and spin doublets (Figs. 4 and 5). We compare eight amplitudes as we consider pair levels. In all four figures, we use dashed lines for the amplitudes with *unnatural* l_z corresponding to the level with Ω, and the dot-dashed lines for the level with $\Omega+1$, respectively. As for the other amplitudes with *natural* l_z, we use solid lines for the level with Ω and dotted lines for the level with $\Omega+1$. Inside the figures, the lines are explained by the asymptotic quantum number $[N,n_z,l_z]\Omega$ together with $\pm$ sign in front of $[N,n_z,l_z]\Omega$, which corresponds to $\pm\frac{1}{2}$ of s_z. The upper components are shown in the left panel, and the lower components are in the right panel in all figures from Figs. 2 to 5.

We adopted the pseudospin doublets with the asymptotic quantum numbers [400]1/2 at -9.109 MeV and [402]3/2 at -9.289 MeV with the energy splitting of 0.180 MeV. In Fig. 2 we show the behavior of the upper components for both levels, i.e., $g^{\Omega}_{\pm,k}$ and $g^{\Omega+1}_{\pm,k'}$ in the left panel, and the lower components, i.e., $f^{\Omega}_{\pm,k}$ and $f^{\Omega+1}_{\pm,k'}$ in the right panel as a function of ρ at $z=3$ fm. We see the values of $g^{\Omega}_{-,k}$ shown by dashed line and $g^{\Omega+1}_{+,k'}$ shown by dot-dashed line in the left panel are almost the same. In the right panel, $f^{\Omega}_{-,k}$ shown by dashed line is the reversal of $f^{\Omega+1}_{+,k'}$ shown by dot-dashed line. They belong to the amplitudes with *unnatural* l_z of pseudospin doublets. In contrast to them, the other amplitudes of pseudospin doublets shown by solid lines and dotted lines give a quite different behavior except for the larger ρ region that are more clearly seen in the left panel. It is marked that the longitudinal scale in the left panel is larger than that in the right panel, which makes us call the upper component as the large component and the lower component as the small component. In order to see the behavior at larger ρ value, we show eight amplitudes for pseudospin doublet ($g^{\Omega}_{\pm,k}$ and $g^{\Omega+1}_{\pm,k'}$, $f^{\Omega}_{\pm,k}$ and $f^{\Omega+1}_{\pm,k'}$) at $\rho=5$ fm as a function of z in Fig. 3. It is seen as good agreement in the absolute values of the amplitudes with *natural* l_z (dashed lines and dot-dashed lines), and also in the amplitudes (solid and dotted lines) in both panels. This is because the centrifugal term in Eq. (2.8) becomes negligible at larger ρ. As is seen from Figs. 2 and 3, the amplitudes with $\tilde{l}_z$ in upper components of the pseudospin doublets are smaller than those with *natural* l_z, and the amplitudes with $\tilde{l}_z$ in lower components of the pseudospin doublet are larger than the other with *natural* l_z.

3. The wave functions for the spin doublet and the triple degeneracy

We choose the spin pair levels of [402]3/2 at -9.289 MeV and [402]5/2 at -10.686 MeV levels. The energy splitting of 1.397 MeV is somewhat large compared with the energy splitting of pseudospin doublet of 0.180 MeV in Fig. 2 and 3, but is still small compared with the other spin pair levels shown in Fig. 6. We show the behaivor of the upper components $g^{\Omega}_{\pm,k}$ and $g^{\Omega+1}_{\pm,k}$ in the left panel, and the lower components $f^{\Omega}_{\pm,k}$ and $f^{\Omega+1}_{\pm,k}$ in the right panel as a function of ρ at $z=1$ fm in Fig. 4. There is a strong agreement on the absolute values of the amplitudes with *natural* l_z of spin doublets, i.e., $g^{\Omega}_{-,k}$ shown by solid lines and $g^{\Omega+1}_{+,k}$ shown by dotted line in the left panel, and $f^{\Omega}_{-,k}$ shown by solid line and $f^{\Omega+1}_{+,k}$ shown by dotted line in the right panel. This figure is comparable to the pseudospin doublet in Fig. 4 in Ref. [9]. In Fig. 5, we show the behaviors of eight amplitudes at

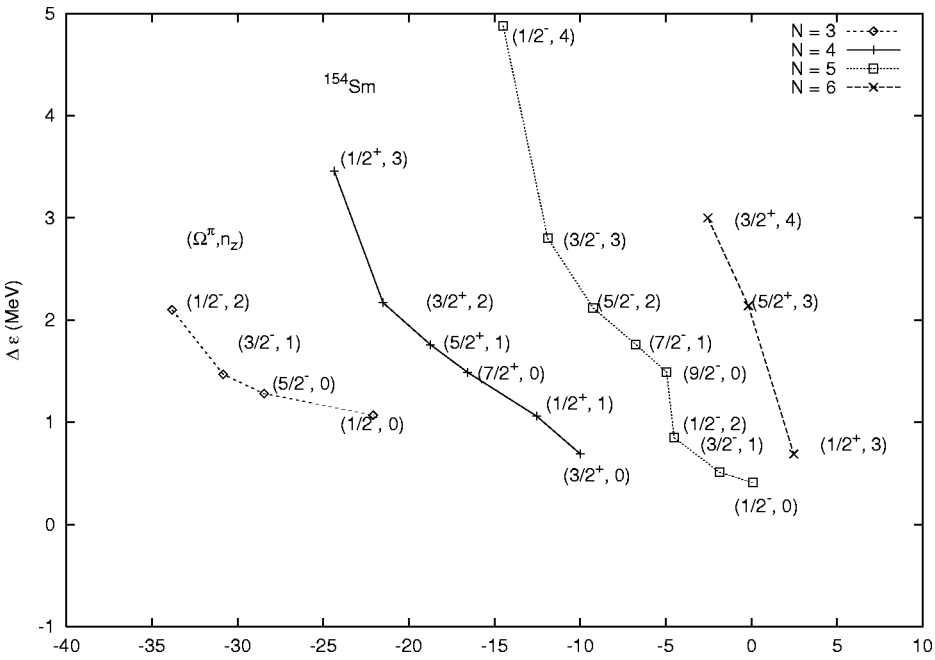

FIG. 7. The energy difference $\Delta\varepsilon$ vs average energy ε for the spin pair levels. The longitudinal axis is for $\Delta\varepsilon$ and the horizontal axis is for ε defined in Eq. (4.2). The numerals inside parentheses are $(\Omega^{\text{parity}},n_z)$. The symbols are the same as defined in Fig. 6.

$\rho=5$ fm as a function of z. It is seen that there is almost total agreement in the absolute values of amplitudes with *natural* l_z (solid and dotted lines) in both panels. As for the amplitudes with *unnatural* l_z (dashed lines and dot-dashed lines), the agreement in the absolute values is unacceptable, but becomes better in the region of large ρ. In contrast to the pseudospin doublets, the amplitudes with *natural* l_z in upper components of the spin doublets are larger than those with *natural* l_z, and the amplitudes with *natural* l_z in lower components of the spin doublets are smaller than those with *unnatural* l_z.

Usually, the spin-orbit force disturbs the degeneracy of spin doublet. However, the result of the relativistic calculation in the spherical case shows that the spin-orbit force is proportional to the potential derivatives, and to l and also inversely to $M+V_S-V_V+\epsilon$ in the denominator. In the deformed case, l is transformed to l_z. As the eigenvalue ϵ is negative and M is positive and much larger than ϵ, the spin-orbit force becomes weaker for the levels not deeply bound with small Ω. Thus, levels such as [402]3/2 and [402]5/2 are less influenced by the spin-orbit interaction and become a spin doublet. On the other hand, [400]1/2 and [402]3/2 are good pseudospin doublets. If both doublets are satisfied, there appears triple degeneracy. The pseudospin doublets and spin doublets, i.e., [400]1/2, [402]3/2, and [402]5/2 levels are good candidates for the triple degeneracy. Although 1.397 MeV and 0.180 MeV are not negligible order, there is no such good candidate with a good triple degeneracy in all the other levels shown in Figs. 6 and 7.

4. The energy splitting of the pseudospin doublet

If we adopt the Nilsson Hamiltonian as a model at the nonrelativistic limit, we can relate $\epsilon_{k,\Omega}$ with the classical energy given by Eq. (5-10) in Bohr-Mottelson's text book [13]. In Fig. 6 we show the value of $\Delta\varepsilon$ as a function of ε. Their definitions in Fig. 6 are as follows:

$$\Delta\varepsilon=\frac{\epsilon_{Nn_zl_z,\Omega}-\epsilon_{Nn_zl_z+2,\Omega+1}}{\tilde{l}_z},$$

$$\varepsilon=\frac{1}{2\tilde{l}_z}[\epsilon_{Nn_zl_z,\Omega}(\tilde{l}_z+1)+\epsilon_{Nn_zl_z+2,\Omega+1}(\tilde{l}_z-1)]. \tag{4.1}$$

By using the same notation as in Eq. (5-10) in Ref. [13], the asymptotic value of $\Delta\varepsilon$ at the nonrelativistic limit is $\hbar\bar{\omega}\tilde{l}_z(v_{ls}-4v_{ll})$ [10]. Here v_{ls} is the strength of the spin-orbit interaction, and v_{ll} is the strength of orbit-orbit interaction at the nonrelativistic limit. In the nonrelativistic treatment, the pseudospin symmetry appears when $v_{ls}\sim 4v_{ll}$, and the asymptotic value of ε in Eq. (4.1) is independent of v_{ls} at the classical limit. The numerals inside the figure are $(\Omega^{\text{parity}},n_z)$, which denote the pair levels with $[N,n_z,l_z]\Omega$ and $[N,n_z,l_z+2](\Omega+1)$ are used for $\Delta\varepsilon$ and ε in Eq. (4.1). The doublets in $N=4$ are shown by plus signs, and the pseudospin doublets for [400]1/2 and [402]3/2 are in the bottom of the chain $N=4$ with suffix $(1/2^+,0)$. The doublets shown by square with $(7/2^-,0)$ are for the levels with [503]7/2 and [505]9/2. The figure shows that $\Delta\varepsilon$ for this doublet is the smallest, but the real energy difference between [503]7/2 and [505]9/2 is 0.279 MeV, which is much larger than the energy difference for [400]1/2 and [402]3/2 of 0.180 MeV. The doublets [400]1/2 and [402]3/2 have the smallest energy splitting in this nucleus.

5. The energy splitting of the spin doublet

Similarly, we show the energy difference $\Delta\varepsilon$ versus ε for the spin doublets in Fig. 7. In this case, the definition of $\Delta\varepsilon$ and ε are as follows:

$$\Delta\varepsilon = \frac{1}{l_z}(\epsilon_{Nn_zl_z,\Omega} - \epsilon_{Nn_zl_z,\Omega+1}),$$

$$\varepsilon = \frac{1}{2}(\epsilon_{Nn_zl_z,\Omega} + \epsilon_{Nn_zl_z,\Omega+1}). \tag{4.2}$$

The asymptotic value of $\Delta\varepsilon$ becomes $\hbar\bar{\omega}v_{ls}$ at the nonrelativistic limit, and the asymptotic value of ε is independent from v_{ls}. Inside the figure, the numerals are also $(\Omega^{\text{parity}},n_z)$, which denote the pair levels with $[N,n_z,l_z]\Omega$ and $[N,n_z,l_z](\Omega+1)$ for $\Delta\varepsilon$ and ε in Eq. (4.2). The spin pair levels of [402]3/2 and [402]5/2 are in the bottom of the $N=4$ chain denoted by plus sign with the suffix of $(3/2^+,0)$. In the figure, the smaller $\Delta\varepsilon$ than the doublets $(3/2^+,0)$ is seen for the doublets in the $N=5$ chain denoted by squares with the sign of $(1/2^-,0)$ and $(3/2^-,1)$. The doublets $(1/2^-,0)$ correspond to the pair levels [501]1/2 and [501]3/2, and $(3/2^-,1)$ to [512]3/2 and [512]5/2. They seem to have a good spin symmetry degeneracy, as energy splitting of $(1/2^-,0)$ is 0.407 MeV and $(3/2^-,1)$ is 1.034 MeV less than 1.397 MeV for $(3/2^+,0)$ in $N=4$ chain. However, their pseudospin partner levels have worse energy degeneracy. For example, the pseudospin doublets of [501]3/2 and [503]5/2, which are pseudospin partners of $(1/2^-,0)$ in Fig. 7, has 0.413 MeV energy splitting. The pseudospin doublets of [510]1/2 and [512]3/2, which are pseudospin partners of $(3/2^-,1)$ in Fig. 7 has 0.252 MeV energy splitting. Both values are much larger than 0.180 MeV for [400]1/2 and [402]3/2. Thus, the candidate for the triple degeneracy in this nucleus is only [400]1/2, [402]3/2, and [402]5/2. The spin symmetry is closely related with the pseudospin symmetry. It is because both the pseudospin symmetry and the spin symmetry are caused as a result of the common spin-orbit interaction.

Now we compare the results in Figs. 6 and 7 with those in the spherical nuclei. In the spherical nuclei, as is seen in Fig. 1 in our previous work [6], $\Delta\varepsilon$ is decreasing for the pseudospin splitting, while $\Delta\varepsilon$ is increasing for the spin-orbit splitting with increasing ε. For the pseudospin doublets in Fig. 6, we see that $\Delta\varepsilon$ is decreasing with increasing ε in the fixed N chain. For example, $\Delta\varepsilon$ in $N=4$ chain decreases with increasing ε starting from $(1/2^+,2)$ to $(1/2^+,0)$. Moreover, if the doublets with the same Ω and its highest n_z chain are connected over different N, their $\Delta\varepsilon$ decrease with increasing ε. For example, $(1/2^-,1)$ in $N=3$, $(1/2^+,2)$ in $N=4$, $(1/2^-,3)$ in $N=5$, and $(1/2^+,4)$ in $N=6$, they are decreasing with increasing energy. Similarly, $(3/2^-,0)$ in $N=3$, $(3/2^+,1)$ in $N=4$,$(3/2^-,2)$ in $N=5$, and $(3/2^+,3)$ in $N=6$ are decreasing. This trend agrees with the spherical case. For the spin doublets $\Delta\varepsilon$ in the fixed N chain decreases with increasing ε. However, if we connect the doublets with the same Ω and its highest n_z over different N, their $\Delta\varepsilon$ increases with increasing ε. For example, $(1/2^-,2)$ in $N=3$, $(1/2^+,3)$ in $N=4$ and $(1/2^-,4)$ in $N=5$, their $\Delta\varepsilon$ are increasing. Similarly, $(3/2^-,1)$ in $N=3$, $(3/2^+,2)$ in $N=4$, and $(3/2^-,3)$ in $N=5$, and $(3/2^+,4)$ in $N=6$ are increasing. Their energy dependence is smaller than the pseudospin doublets. This trend is also found in the spherical case [6].

V. CONCLUSION

We discussed the extreme case where exact pseudospin symmetry and spin symmetry are realized. In that case, the absolute values of amplitudes with *unnatural* l_z in the centrifugal term compared with that estimated from the asymptotic quantum number j_z and s_z agree to each other both in upper (large) and lower (small) components for the pseudospin doublets. On the other hand, for the spin doublets the absolute values of amplitudes with *natural* l_z in the centrifugal term compared with that estimated from the asymptotic quantum number j_z and s_z agree with each other both in upper (large) and lower (small) components. If there were the extreme case, the triple degeneracy appears among the levels with (k,Ω), $(k',\Omega+1)$, and $(k',\Omega+2)$. In the realistic case, we found this situation is almost satisfied for the pseudospin doublets of [400]1/2 and [402]3/2, and for the spin doublets of [402]3/2 and [402]5/2 in ^{154}Sm.

We discussed the relation between the deformed case and the spherical case. In the spherical case, if we transform the cylindrical coordinate to the polar coordinate, the lower (small) component has the pseudospin symmetry, while the upper (large) component has spin symmetry in itself. In contrast to the spherical case the pseudospin and spin symmetries are found both in the upper and lower components in the deformed case. Just as the deformation mixes l and j, the deformation mixes the pseudospin and the spin symmetries. As the pseudospin symmetry is found both in the upper and lower components, it may be the main reason why the pseudospin approximation improves more in the deformed case than in the spherical case.

ACKNOWLEDGMENTS

We are grateful to Professor J. N. Ginocchio for giving us this interesting thema. We thank Professor T. J. Wright for his careful reading of this manuscript.

[1] A. Arima, M. Harvey, and K. Shimizu, Phys. Lett. **30B**, 517 (1969).
[2] K.T. Hecht and A. Adler, Nucl. Phys. **A137**, 129 (1969).
[3] J.N. Ginocchio, Phys. Rev. Lett. **78**, 436 (1997).
[4] J.N. Ginocchio and D.G. Madland, Phys. Rev. C **57**, 1167 (1998); J.N. Ginocchio and A. Leviatan, Phys. Lett. B **425**, 1 (1998).
[5] G.A. Lalazissis, Y.K. Gambir, J.P. Maharana, C.S. Warke, and P. Ring, Phys. Rev. C **58**, R45 (1998).
[6] J. Meng, K. Sugawara-Tanabe, S. Yamaji, P. Ring, and A. Arima, Phys. Rev. C **58**, R628 (1998).
[7] K. Sugawara-Tanabe and A. Arima, Phys. Rev. C **58**, R3065

(1998).

[8] J. Meng, K. Sugawara-Tanabe, S. Yamaji, and A. Arima, Phys. Rev. C **59**, 154 (1999).

[9] K. Sugawara-Tanabe, S. Yamaji, and A. Arima, Phys. Rev. C **62**, 054307 (2000).

[10] R.D. Ratna Raju, J.P. Draayer, and K.T. Hecht, Nucl. Phys. **A202**, 433 (1973); A. Bohr, I. Hamamoto, and B.R. Mottelson, Phys. Scr. **26**, 267 (1982); D. Troltenier, W. Nazarewicz, Z. Szymanski, and J.P. Draayer, Nucl. Phys. **A567**, 591 (1994); A.L. Blokhin, T. Beuschel, J.P. Draayer, and C. Bahri, *ibid.* **A612**, 163 (1997).

[11] K. Sugawara-Tanabe, A. Arima, and N. Yoshida, Phys. Rev. C **51**, 1809 (1995); **53**, 195 (1996).

[12] P. Ring, Y.K. Gambir, and G.A. Lalazissis, Comput. Phys. Commun. **105**, 77 (1997).

[13] A. Bohr and B. R. Mottelson, *Nuclear Structure* (Benjamin, New York, 1975), Vol. 2, p. 224.